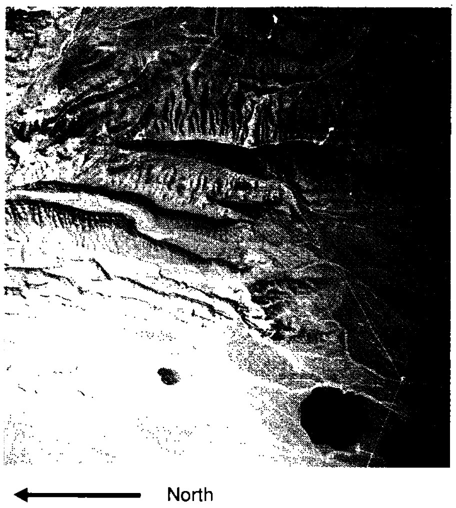

Fig. 7. Air photo of the Yucca Mountain area of southern Nevada and small-scale interaction between normal faulting and magmatic activity. The scarps of active normal faults strike toward the basaltic cones in the lower right corner, where the faults die out. Increased local magmatic input to the crust is absorbing the extension that otherwise would be accommodated by these faults.

gous regions that have holes, or low-seismic zones in the pattern of seismicity are scattered around the Basin and Range Province. The Yucca Mountain area of southern Nevada (Fig. 7), the Mono Craters of eastern California (*28*), and the Valles Caldera of New Mexico (*29*) all show a relation between young magmatism and low seismicity. Vertical intrusions are observed to be accommodating extensional strain in the Coso Mountains of California (*30, 31*).

When assessing volcanic and earthquake hazards it is important to recognize that these phenomena often occur as coupled processes and that magmatism plays an important role in relieving tectonic stresses, particularly in extending regimes. Geophysical remote sensing methods capable of detecting horizontal magmatic intrusions, as well as in situ stress measurements, offer a means of confirmation where magmatic stress accommodation is suspected. An understanding of dike and sheet emplacement may also be important for controlling massive artificial hydrofracturing, which is often used to enhance the yield of oil from reservoirs.

REFERENCES AND NOTES

1. See S. I. Kirby and A. K. Kronenberg, *Rev. Geophys.* **25**, 1219 (1987), for review and detailed references on crustal rheology.
2. M. G. Best, *Igneous and Metamorphic Petrology* (Freeman, New York, 1982).
3. S. H. Emerman and R. Marrett, *Geology* **18**, 231 (1990).
4. For simplicity we describe the stresses as if they were uniform over broad regions. We recognize, however, that dikes propagate because of the extremely nonuniform stresses at their tips [see (*5*) and D. Moos and M. D. Zoback, *J. Geophys. Res.* **95**, 9305 (1990)]. We generally do not include pore pressure in the discussion because magma does not appreciably penetrate rock pores, but in the zone of melt generation internal pore pressure of the melt fraction can reduce the effective stress and cause rocks at great depth to behave in brittle fashion.
5. A. M. Rubin and D. D. Pollard, *Geology* **16**, 413 (1988).
6. E. M. Anderson, *The Dynamics of Faulting and Dyke Formation* (Oliver and Boyd, Edinburgh, 1951).
7. M. K. Hubbert and D. G. Willis, *Trans. Am. Inst. Min. Metall. Pet. Eng.* **210**, 153 (1957).
8. N. H. Sleep, *J. Geophys. Res.* **93**, 10,225 (1988).
9. D. L. Turcotte and G. Schubert, *Geodynamics* (Wiley, New York, 1982), p. 240.
10. Intentionally not discussed here are effects of viscous loss associated with fluid flow and local stress effects associated with crack propagation such as opening and healing. Although these effects are important to understanding dike emplacement, they are of secondary importance in their contribution to the overall stress field that governs faulting, earthquakes, and topography.
11. C. Juhlin, in *Deep Drilling in Crystalline Bedrock*, A. Boden and K. G. Eriksson, Eds. (Springer-Verlag, New York, 1988), pp. 113–121.
12. E. Goodwin *et al.*, *Tectonics* **8**, 821 (1989).
13. J. McCarthy and G. A. Thompson, *Geol. Soc. Am. Bull.* **100**, 1361 (1988).
14. J. M. Howie, T. Parsons, G. A. Thompson, in *Fourth International Symposium on Deep Seismic Reflection Profiling of the Continental Lithosphere*, R. Meissner and H. Dürbaum, Eds. (*Geophys. Monog. 63*, American Geophysical Union, Washington, DC, in press).
15. C. E. Corry, *Geol. Soc. Am. Spec. Pap.* **220**, 1 (1988).
16. K. A. Howard, *J. Geophys. Res.*, in press.
17. B. Gutenberg and C. F. Richter, *Seismicity of the Earth* (Princeton Univ. Press, Princeton, NJ, ed. 2, 1954).
18. K. C. Macdonald and J. D. Mudie, *Geophys. J. R. Astron. Soc.* **36**, 245 (1974).
19. T. Simkin, R. I. Tilling, J. N. Taggart, W. J. Jones, H. Spall, *This Dynamic Planet, Volcanoes, Earthquakes, and Plate Tectonics* (Smithsonian Institution, Washington, DC, 1989).
20. B. Isacks, J. E. Oliver, L. R. Sykes, *J. Geophys. Res.* **73**, 5855 (1968).
21. W. J. Morgan, *Am. Assoc. Pet. Geol. Bull.* **56**, 230 (1972).
22. R. B. Smith and M. L. Sbar, *Geol. Soc. Am. Bull.* **85**, 1205 (1974).
23. F. C. Armstrong, W. P. Leeman, H. E. Malde, *Am. J. Sci.* **275**, 225 (1975).
24. M. H. Anders, J. W. Geissman, L. A. Piety, J. T. Sullivan, *J. Geophys. Res.* **94**, 1589 (1989).
25. R. B. Smith, W. D. Richins, D. I. Doser, *U.S. Geol. Surv. Open-File Rep.* **85-290**, 236 (1985).
26. D. W. Rodgers, W. R. Hackett, H. T. Ore, *Geology* **18**, 1138 (1990).
27. W. R. Hackett, R. P. Smith, S. M. Jackson, in preparation.
28. M. Bursik and K. Sieh, *J. Geophys. Res.* **94**, 15,587 (1989).
29. D. J. Cash and J. J. Wolff, in *Guidebook, 35th Field Conference, Rio Grande Rift: Northern New Mexico*, W. S. Baldridge, P. W. Dickerson, R. E. Riecker, J. Zidek, Eds. (New Mexico Geological Society, Socorro, 1984), pp. 25–28.
30. C. R. Bacon, *Geology* **10**, 65 (1982).
31. ———, *Geol. Soc. Am. Abstr. Program.* **15**, 288 (1988).
32. G. P. Thelin and R. Pike, *U.S. Geol. Surv. Map 12206*, in press.
33. R. Pike and G. Thelin provided their digital topographic map of the western United States (*32*) for use in figures appearing in this paper. The U.S. Department of Energy provided air photos of Yucca Mountain, NV. We thank R. Smith, W. Hackett, and S. Jackson at Idaho National Engineering Labs for cooperative discussions on crustal processes of the Snake River Plain. Thanks also to N. Sleep and the Crustal Geophysics group at Stanford for helpful discussion. This work was funded by National Science Foundation grant EAR 9017667.

7 May 1991; accepted 23 July 1991

Soil Carbon Isotope Evidence for Holocene Habitat Change in the Kenya Rift Valley

STANLEY H. AMBROSE AND NANCY E. SIKES

In eastern Africa the altitude of the boundary between montane forest and lowland savanna grassland changed substantially in response to climate change during the later Holocene, but this is not clearly reflected in regional pollen records. The carbon-13 to carbon-12 ratios of tropical grasses are higher than those of most other plants, and this difference is preserved in soil organic carbon stable isotope ratios. Soil organic matter $^{13}C/^{12}C$ ratios in profiles along an altitude transect in the central Rift Valley of Kenya suggest that the forest-savanna boundary advanced more than 300 meters in altitude. This could have implications for understanding the effects of climate change on the configuration of floral zones, prehistoric hunter-gatherer land-use patterns, and the timing of the advent of Neolithic food production.

CHANGES IN FLORAL ZONES IN East Africa during the late Quaternary have been shown by analyses of pollen from cores in swamps and lakes (*1*). Pollen provides taxonomic identifications of the composition of plant communities, but the precise location of the boundaries between major floral zones cannot be determined because of the size and altitudinal range of pollen site catchment areas. Direct identification of the past position of the boundary (ecotone) between forest and savanna in the central Rift Valley of Kenya would permit a test of arguments that the boundary was at higher altitudes during a middle Holocene arid phase; it would allow us to test a model of prehistoric human forager ecotonal settlement preferences (*2, 3*). The stable carbon isotope ratios of soil and paleosol organic matter are lower in forests than in tropical grasslands. Past changes in the position of the forest-savanna ecotone can thus be doc-

---

Department of Anthropology, University of Illinois, Urbana, IL 61801.

umented by isotopic analysis of soils (*4, 5*).

Plants with the C_3 photosynthetic pathway (trees, shrubs, and high-latitude and high-altitude grasses) have $\delta^{13}C$ values (*6*) between −22 and −35 per mil, with a mean of −26.5 per mil (*7*). C_4 plants (most tropical grasses and some pioneering weeds) have $\delta^{13}C$ values between −8 and −16 per mil, with a mean of −12.5 per mil (*7*). C_4 plants thrive at high temperatures in strong sunlight, but are replaced by C_3 plants in cool, moist, and shaded areas such as forests, winter rainfall zones, high latitudes, and high altitudes (*8, 9*). At the equator the C_4/C_3 grass flora transition zone occurs between 2000 and 3100 m (*9*). Forest plant biomass is almost entirely C_3, and savanna grassland biomass is mainly C_4.

Soil organic carbon is derived mainly from plants and thus has a $\delta^{13}C$ value that closely reflects that of the standing plant biomass (*4, 5*). There may be enrichment of +1 to +3 per mil in soil $\delta^{13}C$ values relative to those of plants (*10*), but this cannot mask the 14 per mil mean difference between C_3 and C_4 floras. Therefore the proportions of C_3 versus C_4 plant biomass can be accurately determined from the $\delta^{13}C$ value of soil organic carbon (*4, 5*).

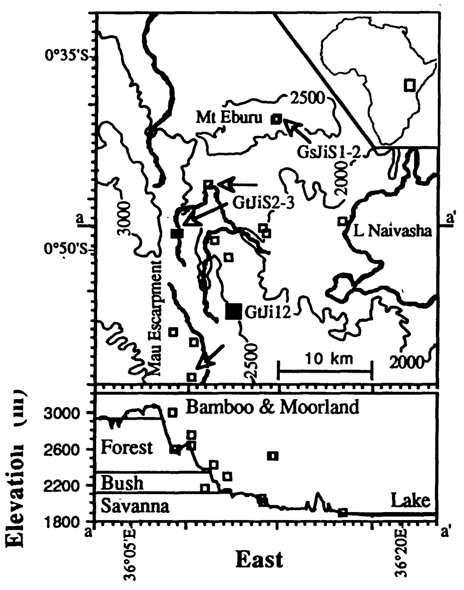

Fig. 1. The Naivasha Basin, showing elevation contours at 500-m intervals, permanent streams and lakes, soil and plant sampling sites, and rock-shelter site Enkapune Ya Muto (GtJi12). Arrows point to forest sites that show substantial changes in soil organic carbon $\delta^{13}C$ values below the surface. Sites whose $\delta^{13}C$ values are shown in Fig. 3 are indicated. The altitudinal positions of the sites relative to floral zones along an east-west transect between points a-a' are shown below the map. The major floral zones are *Acacia xanthophloea* woodland and forest in the lake margin zone (1890 to 1900 m), open to wooded *Acacia* spp. and *Tarchonanthus camphoratus* savanna grasslands (1900 to 2000 m), *Tarchonanthus*, *Acacia*, and *Olea africana* bush (2000 to 2300 m), dry montane *Juniperus procera* and *Podocarpus* spp. forest (2300 to 2700 m), and open grassy moorlands with *Hagenia abyssinica* trees and patches of forest and bamboo (2700 to 3100 m).

In the Kenya Rift Valley five floral zones occur between the shore of Lake Naivasha and the crest of the Mau Escarpment (Fig. 1). The altitudinal boundaries of these zones vary depending on slope, aspect, disturbance, and edaphic conditions (*11*). The forest-savanna ecotone occurs between 2300 and 2500 m. Within the forest there are several small isolated patches (<1 km^2) and two larger valley floors with open grassland.

Thirteen 55-cm-deep pits were excavated along an altitude transect from 1890 to 2990 m (Fig. 2). The pits were located away from termite mounds, archeological sites, and recent human disturbance. All soils were weakly developed, with only slight color changes, no obvious zones of eluviation or illuviation, and little observable structure. Earthworms, termite nests, rodent burrows, and pedogenic carbonate nodules were not observed. The mean $\delta^{13}C$ value of leaves of 102 C_3 plants collected in the immediate vicinity of the soil sites is −26.8 ± 1.9 per mil (1 SD) and that of 14 C_4 plants (grasses) is −11.6 ± 0.9 per mil. These mean values provide local end points for estimating the proportions of C_3 and C_4 plant biomass from soil carbon isotope ratios.

Humic acids (*12*) from the 0- to 5-cm level at four sites in montane forest have $\delta^{13}C$ values of −24 to −26 per mil, and that of an open grassland site at 2600 m is −11.9 per mil (Fig. 2), representing 1 to 10% and approximately 95% C_4 plant biomass, respectively. A forest site with a grassy understory (GsJiS3, at 2160 m) has a $\delta^{13}C$ value of −21 per mil, indicating ~30% C_4 plant biomass. Seven sites in bush or wooded grassland have $\delta^{13}C$ values that indicate between 45 and 80% C_4 plant biomass. Profiles in bush and open grasslands maintain high (less negative) $\delta^{13}C$ values, and one in forest at 2990 m maintains low values below the surface. The plant communities at these sites have thus been relatively stable through the time span represented by 55 cm of soil formation. Four sites that are now in forest have high $\delta^{13}C$ values at the 35- to 55-cm levels, indicating they previously supported approximately 50 to 75% C_4 plants.

Figure 3 shows the $\delta^{13}C$ values of whole soils and humic acids for adjacent sites in open grassland and montane forest (*13*). The pronounced shift to less negative soil $\delta^{13}C$ values below the surface in four forest sites cannot be explained by downward transport of ^{13}C-rich organic matter because the current source of organic carbon is a C_3 flora. Some downward and upward transport of soil organic matter undoubtedly occurred. Therefore the surface and subsurface soil $\delta^{13}C$ values in the forested sites with substantial isotopic shifts should be considered minimum estimates of the past abundance, and maximum estimates of the present abundance of C_4 plants. High soil $\delta^{13}C$ values at 35 to 55 cm in four forest sites demonstrate that the savanna-forest ecotone was located somewhere between 2630 and 2990 m during the recent past, probably during a period of drier climate. The four sites are separated from each other

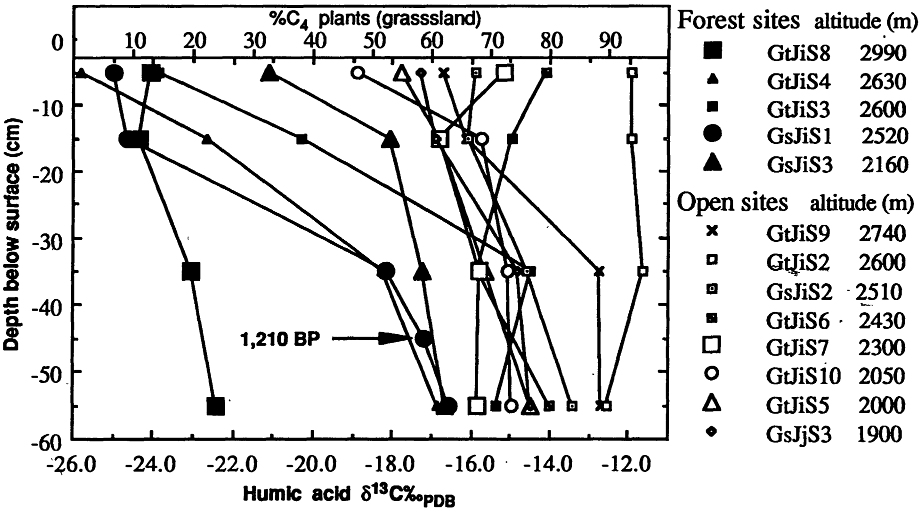

Fig. 2. Humic acid $\delta^{13}C$ values for 13 soil profiles sampled at four or more levels below the surface (0 to 5, 10 to 15, 30 to 35, 40 to 45, and 50 to 55 cm). The upper horizontal scale indicates the equivalent percentage of C_4 flora, assuming a +1 per mil enrichment in soil relative to plant $\delta^{13}C$ values (*10*). The end point $\delta^{13}C$ values are set at −26 per mil for 100% C_3 (forest) and −11 per mil for 100% C_4 (grassland).

by almost 30 km (Fig. 1), demonstrating that this is a regional phenomenon.

Radiocarbon dating provides a minimum estimate of the age of the period of reduced forest cover. Humic acids from the 40- to 45-cm level of one forest profile (GsJiS1) date to 1210 ± 100 years before present (BP) (ISGS-1922), and humin dates to 1180 ± 90 BP (ISGS-1923). Despite the carbon isotopic evidence for relatively little soil mixing, these dates must be considered minimum estimates of the age of this level because bioturbation, organic carbon labeled with bomb ^{14}C, rootlet contamination, and oxidation of older carbon will significantly decrease the apparent age (*14*). Limnological and palynological evidence for the timing of climatic changes suggests that the grassland expansion dates to a period of drier climate between 5600 or 4000 and 3000 BP (*15, 16*). Central Rift lakes dried up completely between 3400 and 3000 BP (*17*). With the exception of sites in southwest Uganda (*18, 19*), East African pollen records indicate a climate as dry as, or only slightly drier than at present, after 3800 BP (*1*). Soil carbon isotope ratios reported here thus provide the most direct evidence for the mid-Holocene rise in the altitude of the savanna-forest ecotone in the central Rift Valley.

The mid-Holocene dry phase had a significant impact on prehistoric human populations (*2, 3*). A pronounced gap in the archeological sequence between 6000 and 3300 BP in the Kenya and northern Tanzania highlands spans the transition from foraging to food production (*2*). Modern Okiek hunter-gatherers in this region preferred to settle on the forest-savanna ecotone (*20*). If pre-Neolithic foragers also preferred this ecotone then the gap could reflect a shift to poorly investigated higher altitudes (*2, 3*). Eburran Industry sites dating to the early Holocene wet phase are all located below 2000 m and contain forest and savanna faunas (*21, 22*). At rock-shelter site Enkapune Ya Muto (Fig. 1), fauna, site-use patterns (*21, 23*), and herbivore tooth carbon and nitrogen isotope ratios (*24*), indicate that the ecotone was below this site before 5400 BP, in the site's vicinity between 5400 and 4400 BP (during the period of highest occupation intensity), and above the site between 4400 and 2600 BP. These data suggest that the forest-savanna ecotone was the preferred zone of Eburran hunter-gatherer occupation, and that it rose from below 2000 m to over 2400 m between the early and middle Holocene.

The mid-Holocene dry phase is only documented clearly in swamps in southwest Uganda, which show an increase in grass pollen, sediment $\delta^{13}C$ values, and charcoal after 3800 BP (*18*). An alternative interpretation for this change is forest clearance and disturbance by Neolithic agriculturalists (*19*). There is, however, no archeological evidence for Neolithic occupation of southwest Uganda. In the Kenya and Tanzania highlands mid-Holocene sites are extremely rare and contain scant evidence for food production (*2, 23*). Neolithic sites are abundant after 3000 BP, when soil carbon isotope evidence suggests reforestation. The archeological evidence is inconsistent with an anthropogenic cause for mid-Holocene deforestation in the Rift Valley and casts doubt upon this explanation in southwest Uganda.

Soil organic carbon isotopic evidence for the effects of climate change on the position of the savanna-montane forest ecotone in the Kenya Rift Valley clarifies our understanding of environmental influences on changes in hunter-gatherer settlement locations and the timing of the advent of food production. This method can be used for mapping of the past distribution and changes in proportions of C_3 and C_4 microhabitats in response to climate change (*5, 25*) and habitat variation along isochronous horizons of paleolandscapes (*26*).

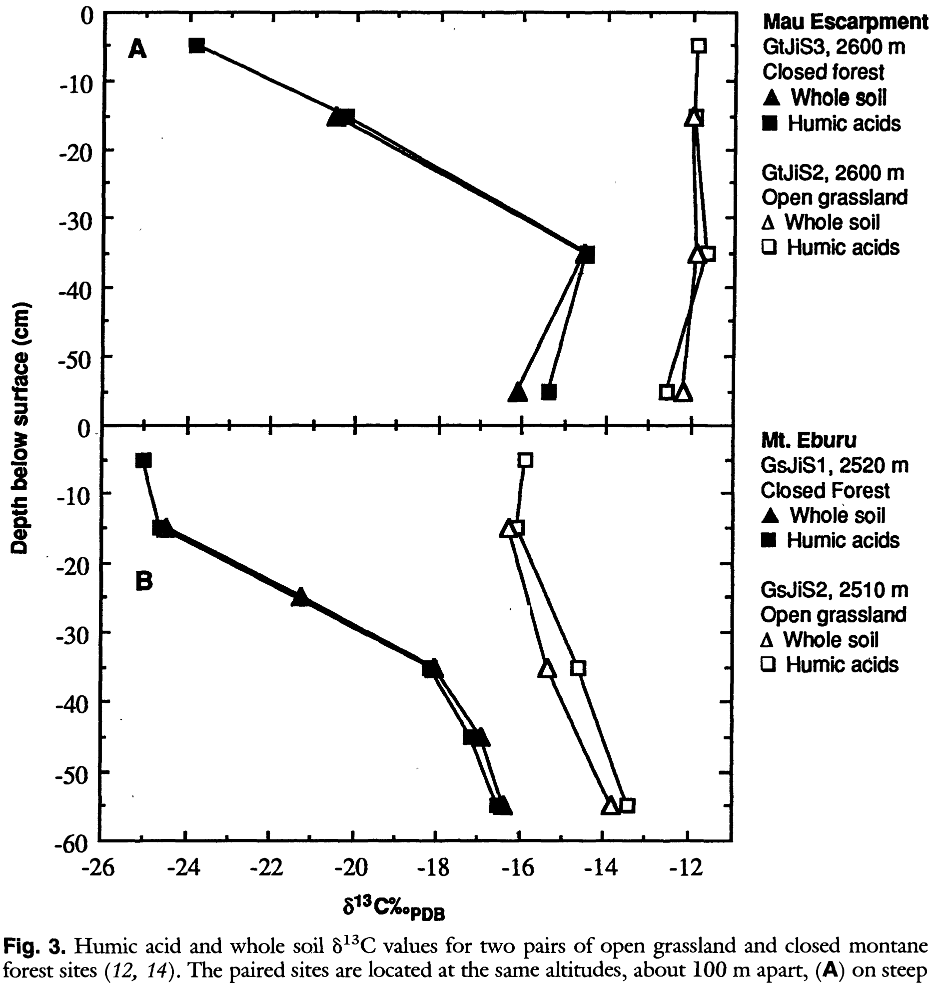

Fig. 3. Humic acid and whole soil $\delta^{13}C$ values for two pairs of open grassland and closed montane forest sites (*12, 14*). The paired sites are located at the same altitudes, about 100 m apart, (**A**) on steep slopes on the Mau Escarpment (sites GtJiS2 and S3) and (**B**) on nearly level ground near the summit of Mt. Eburu (GsJiS1 and S2).

REFERENCES AND NOTES

1. A. C. Hamilton, *Environmental History of East Africa* (Academic Press, London, 1982).
2. S. H. Ambrose, in *From Hunters to Farmers*, J. D. Clark and S. A. Brandt, Eds. (Univ. of California Press, Berkeley, 1984), pp. 219–239.
3. _____, *Sprache und Geschichte in Afrika* 7 (2), 11 (1986).
4. J. Balesdent *et al.*, *Soil Biol. Biochem.* **19**, 25 (1987); A. Martin *et al.*, *ibid.* **22**, 517 (1990).
5. T. E. Cerling, J. Quade, Y. Wang, J. R. Bowman, *Nature* **341**, 138 (1989); B. Guillet, P. Faivre, A. Mariotti, J. Khobzi, *Palaeogeogr. Palaeoclimatol. Palaeoecol.* **65**, 51 (1988); T. E. Cerling, J. Quade, S. H. Ambrose, N. E. Sikes, *J. Hum. Evol.*, in press.
6. $\delta^{13}C$ per mil is defined as $[\{(^{13}C/^{12}C)_{sample}/(^{13}C/^{12}C)_{standard}\}^{-1}] \times 1000$. The standard is the PDB marine fossil carbonate.
7. B. N. Smith, *BioScience* **22**, 226 (1972).
8. J. C. Vogel, A. Fuls, R. P. Ellis, *S. Afr. J. Sci.* **75**, 209 (1978).
9. D. A. Livingstone and W. D. Clayton, *Quat. Res.* **13**, 392 (1980); L. L. Tieszen *et al.*, *Oecologia* **37**, 337 (1979).
10. S. J. Ladyman and D. D. Harkness, *Radiocarbon* **22**, 885 (1980); P. Becker-Heidmann and H-W. Scharpenseel, *Radiocarbon* **28**, 383 (1986).
11. E. M. Lind and M. E. S. Morrison, *East African*

Vegetation (Longman, London, 1974).

12. Soil fractions were prepared as follows: macroscopic organic matter was removed by hand, the soil gently ground in a mortar, and sieved. The <355-μm fraction (10 g) was treated with 1 M HCl at 25°C for 15 hours and rinsed to pH 3 by centrifugation with distilled water. Carbonate-free whole soil (1 g) was reserved; the remainder was treated with 50 ml of 0.125 M NaOH for 15 hours at 25°C, with constant agitation on a reciprocal shaker. The supernatant (humic acids) was reserved, and the treatment repeated. The residue (humin) was rinsed, acidified, rinsed to pH 3, and freeze-dried. The humic acid supernatants were precipitated by titration with HCl, centrifuged, and the residue rinsed to pH 3. This residue was redissolved in 25 ml of 0.125 M NaOH, centrifuged, and any pellet was discarded. The supernatant (purified humic acids) was reprecipitated, rinsed to pH 3, and freeze-dried. Plant leaves were sonicated in distilled water, dried at 70°C, and ground in a Wiley Mill. Organic carbon was converted to CO_2 by sealed tube combustion with CuO, Cu, and Ag foil for 3 hours at 860°C. The precision of $\delta^{13}C$ analysis is ±0.1 per mil (1 SD).
13. The $\delta^{13}C$ values of 41 paired whole soil and humic acid fractions are correlated ($r^2 = 0.988$); their mean difference is 0.09 ± 0.36 per mil (1 SD).
14. J. A. Matthews, in *Geomorphology and Soils*, K. S. Richards, R. R. Arnett, S. Ellis, Eds. (Allen & Unwin, London, 1985), pp. 269–288.
15. K. W. Butzer, G. L. Isaac, J. L. Richardson, C. K. Washbourne-Kamau, *Science* **175**, 1069 (1972).
16. J. L. Richardson and A. E. Richardson, *Ecol. Monogr.* **42**, 499 (1972); J. L. Richardson and R. A. Dussinger, *Hydrobiologia* **143**, 167 (1986); J. M. Maitima, *Quat. Res.* **35**, 234 (1991).
17. J. L. Richardson, *Palaeoecol. Africa* **6**, 131 (1972).
18. R. A. Perrott, *Nature* **325**, 89 (1987); D. M. Taylor, *Palaeogeogr. Palaeoclimatol. Palaeoecol.* **80**, 283 (1990).
19. A. C. Hamilton, D. Taylor, J. C. Vogel, *Nature* **320**, 164 (1986); in *Quaternary and Environmental Research on East African Mountains*, W. C. Mahaney, Ed. (Balkema, Rotterdam, 1989), pp. 435–463.
20. R. H. Blackburn, in *Politics and History in Band Societies*, R. B. Lee and E. Leacock, Eds. (Cambridge Univ. Press, Cambridge, 1982), pp. 283–305.
21. S. H. Ambrose, thesis, University of California, Berkeley (1984).
22. D. P. Gifford-González, *Azania* **20**, 69 (1985).
23. C. W. Marean, thesis, University of California, Berkeley (1990).
24. S. H. Ambrose and M. J. DeNiro, *Quat Res.* **31**, 407 (1989).
25. D. Schwartz, A. Mariotti, R. Lanfranchi, B. Guillet, *Geoderma* **39**, 97 (1986); J. Quade, T. E. Cerling, J. R. Bowman, *Nature* **342**, 163 (1989).
26. R. S. Dzurec *et al.*, *Oecologia* **66**, 17 (1985).
27. We thank the Office of the President and the National Museums of Kenya for permission to conduct field research and J. Hayes, C. Kabuye, and the staff of the East African Herbarium for plant identifications. T. Anderson, T. Cerling, T. Dillehay, D. Gillieson, L. Follmer, D. Johnson, and L. Norr provided useful comments. Supported by NSF grant BNS 87-07150 and the University of Illinois Research Board.

22 January 1991; accepted 12 June 1991

Atomic Force Microscopy and Dissection of Gap Junctions

JAN H. HOH, RATNESHWAR LAL,* SCOTT A. JOHN, JEAN-PAUL REVEL, MORTON F. ARNSDORF

An atomic force microscope (AFM) was used to study the structure of isolated hepatic gap junctions in phosphate-buffered saline (PBS). The thickness of these gap junctions appears to be 14.4 nanometers, close to the dimensions reported by electron microscopy (EM). When an increasing force is applied to the microscope tip, the top membrane of the gap junction can be "dissected" away, leaving the extracellular domains of the bottom membrane exposed. When such "force dissection" is performed on samples both trypsinized and fixed with glutaraldehyde, the hexagonal array of gap junction hemichannels is revealed, with a center-to-center spacing of 9.1 nanometers.

GAP JUNCTIONS CONSIST OF TWO apposed plasma membranes that contain an array of cell to cell channels (*1*). These channels form aqueous pores that allow the free passage of small molecules (<1 kD) in vertebrates and provide a low-resistance electrical pathway between cells (*2*). Proposed biological functions for gap junctions include regulation of growth, transmission of developmental signals, coordination of smooth muscle contraction, synchronization of myocardial contractions, and maintenance of metabolic homeostasis (*3*).

The structure of the gap junction has been studied extensively by physical and biochemical methods. It was first described by EM as a close membrane apposition (*4*) with a quasi-crystalline array of particles (*5*), and subsequently a gap between the membranes was defined (*1*). Models of the gap junction have been constructed with data from x-ray diffraction, EM, and Fourier-based three-dimensional reconstruction techniques (*6*, *7*). In the current model, the gap junction is composed of two apposed membranes with a 2- to 3-nm gap between them and a closely packed array of cell-cell channels. The most regular samples show hexagonal packing with a lattice constant of 8 to 10 nm, but the degree of order varies depending on the preparation. Each channel is composed of two connexons, one from each membrane, aligned head-to-head across the gap. The connexon is shaped roughly as a cylinder 7.5 nm in height and 7 nm in diameter, with a 1.5- to 2.0-nm pore through the center. Each connexon exhibits sixfold symmetry and is thought to consist of six identical or homologous protein subunits.

The AFM has been used to image a number of biological specimens (*8*–*10*). Details of the operation of AFMs have been presented (*8*, *11*, *12*). We have used an AFM equipped with a fluid cell to probe the structure and organization of isolated gap junctions adsorbed to glass in PBS (*13*), and we have also used the AFM to manipulate these membranes.

Gap junctions from rat liver were isolated as membrane pairs, often referred to as plaques, with densely packed cell to cell channels (*14*). These plaques, imaged under PBS by atomic force microscopy, appear to be similar in general shape and distribution to ones seen by EM (Fig. 1, A and B). They are flat structures, 0.5 to 1 μm in size, with irregular edges and are 14.4 nm thick (Fig. 1C). Occasionally a step of 6 to 7 nm is seen at the edge of a plaque that either represents a single membrane from a gap junctional plaque or a piece of nonjunctional membrane attached to the gap junction. The surface of the gap junction has height variations of ~1 nm, but sometimes bumps 50 to 100 nm in width and several nanometers in height are seen. At high magnification, the surface has no discernible regular features and is smoothly undulating. High-magnification images of the glass itself are remarkably smooth, with z variation of only 1 to 2 nm and no detectable regular pattern (Fig. 1D).

Glutaraldehyde fixation of hepatic gap junctions does not result in any discernible changes in morphology. Interestingly, all of the samples that were glutaraldehyde-fixed were more easily scraped off the glass substrate. This result may be attributable to the reaction of glutaraldehyde with amino groups of molecules such as phospholipids and proteins. Reaction of these molecules with glutaraldehyde would reduce the total positive charge of the gap junction membrane and thereby reduce the strength of the electrostatic interactions between the gap junction and the negatively charged glass. The adsorption of purple membranes to mica requires positively charged membranes (*10*).

We examined the effect of force on the structure and appearance of the gap junction. Samples were imaged in PBS in an increasing force series from less than 1 nanonewton (nN) to ~15 nN. After a gap

---

J. H. Hoh, S. A. John, J.-P. Revel, Division of Biology, California Institute of Technology, Pasadena, CA 91125.
R. Lal and M. F. Arnsdorf, Section of Cardiology, Department of Medicine, University of Chicago, Chicago, IL 60637.

*To whom correspondence should be addressed.